

Study of the Solubility of Iron Carbonate in the Presence of Acetic Acid using an EQCM

Vanessa Fajardo, Bruce Brown, David Young, Srdjan Nešić
Institute for Corrosion and Multiphase Technology
Department of Chemical & Biomolecular Engineering
Ohio University
342 West State St., Athens, OH 45701
United States

ABSTRACT

This research aims to study the solubility of a protective iron carbonate (FeCO_3) layer in the presence of acetic acid using an electrochemical quartz crystal microbalance (EQCM). Several sets of experiments were conducted *in situ* to quantitatively evaluate the solubility of an FeCO_3 layer in the presence of acetic acid. The first set of experiments was designed to determine the influence of the pH on FeCO_3 precipitation in the absence of acetic acid. The second set of experiments to study the solubility of the FeCO_3 layer was conducted with three different undissociated acetic acid concentrations (1mM, 3mM, and 5mM) at pH 6.0 and 80°C. The acetic acid was added into the system as a buffered solution for each test so no change in pH occurred. After each test, the corrosion product film was characterized by SEM, EDX/EDS, Raman spectroscopy, XPS, and TEM surface analysis techniques. From both series of tests, it was proven that the presence of acetic acid partially removed the FeCO_3 layer by selective dissolution.

Key words: platinum coated quartz crystal, iron carbonate, acetic acid, EQCM, SEM, EDS, FIB/TEM/ED, diffraction, XPS

INTRODUCTION

Mild steel exposed to aqueous CO_2 solutions may corrode rapidly unless a protective FeCO_3 layer develops, typically at higher pH (>pH6) and higher temperature ($T > 60^\circ\text{C}$). This layer offers protection to the steel by being a diffusion barrier for cathodic species and by covering the steel surface and blocking the iron dissolution reaction. It can be readily removed when the solution becomes more acidic and the pH drops below the saturation level for FeCO_3 , what may lead to very high corrosion rates and often result in severe localized attack. Furthermore, some previous studies¹ have shown that FeCO_3 can be lost from the steel surface due to the action of acetic acid (CH_3COOH or shortly HAc), even if the solution remains supersaturated with respect to FeCO_3 . It has been speculated that this loss can happen for the two following reasons:

- a) Undermining – acetic acid diffuses through the pores of the FeCO_3 layer and directly attacks the steel underneath resulting in loss of FeCO_3 adherence
- b) Selective dissolution of FeCO_3 – acetic acid has a preference for certain FeCO_3 crystal morphologies that it can more readily dissolve.

In the previous work, the loss of the FeCO_3 was only detected after the completion of the experiments i.e. when the steel samples were analyzed using a range of techniques such as scanning electrode microscopy (SEM) and energy-dispersive X-ray spectroscopy (EDX/EDS). In order to better characterize this behavior, it was thought to be beneficial to make use of an *in situ* mass loss detection device: an EQCM. In the present study, several sets of experiments were conducted with this instrument in order to quantitatively evaluate the solubility of an FeCO_3 layer in the presence of acetic acid, *in situ*.

EXPERIMENTAL PROCEDURE

A three-electrode setup was used in all the experiments (Figure 1). A platinum-coated quartz crystal was used as the working electrode (WE). Platinum wire was used as a counter electrode (CE) with a saturated silver-silver chloride (Ag/AgCl) reference electrode (RE). The glass cell was filled with 2 liters of 0.1 wt.% NaCl electrolyte and heated to 80°C (pH was adjusted to 6.0 with NaHCO_3). In all experiments, CO_2 was continuously bubbled through the electrolyte for approximately 1 hour before the experiment and during the entire experiment. The platinum coated quartz crystal was used and as a substrate to form the FeCO_3 layer, and it was polarized to -700mV to mimic the corrosion potential of steel in CO_2 solutions and to facilitate the FeCO_3 precipitation. Moreover, using platinum substrate enabled the FeCO_3 dissolution experiments to be done without any interference by corrosion of the underlying steel. Even if it appears more appropriate, using an iron coated quartz crystals was found to be impractical for a number of reasons: 1) the thickness of an iron coated quartz crystal used in previous precipitation studies was around $1\mu\text{m}^2$ and therefore would corrode away before the precipitation of FeCO_3 was complete; 2) the surface of the iron coated quartz crystal surface was too smooth which inhibited the nucleation process of FeCO_3 which precedes any crystal growth during precipitation; and 3) it was difficult to differentiate the mass loss due to the corrosion process from the mass loss resulting from FeCO_3 dissolution, as both processes occur simultaneously.

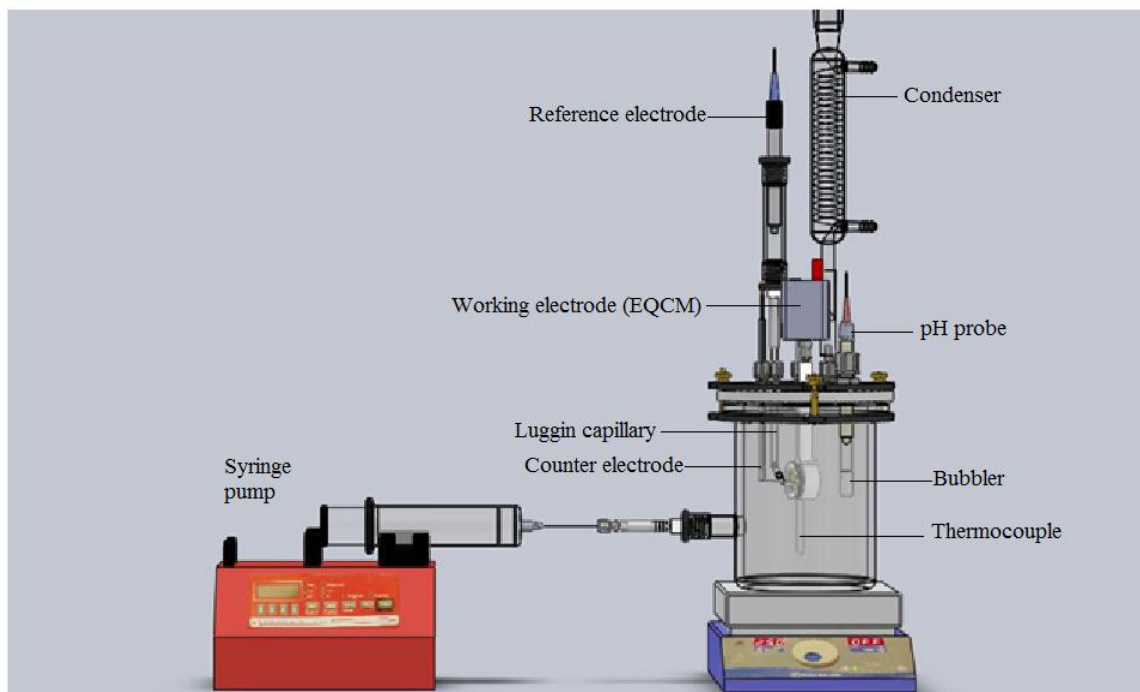


Figure 1: Experimental cell design used to measure the solubility of the FeCO_3 layer.

Several sets of experiments were conducted to evaluate the solubility of the FeCO₃ layer in the presence of acetic acid using the EQCM. Surface analyses were performed with scanning electrode microscopy (SEM), energy-dispersive X-ray spectroscopy (EDX/EDS), Raman spectroscopy and X-ray photoelectron spectroscopy (XPS).

The first set of experiments was designed to determine the influence of the pH on FeCO₃ precipitation in the absence of acetic acid (Table 1). High initial FeCO₃ supersaturation (>100) was achieved by using FeCl₂ addition in order to accelerate FeCO₃ formation. The second set of experiments were carried out to study the solubility of the FeCO₃ layer in the presence of acetic acid by using three different undissociated acetic acid concentrations of 1, 3, and 5mM at pH 6.0 and 80°C (see Table 2). The acetic acid was added into the system only after a stable protective FeCO₃ layer formed on the platinum coated quartz crystal, as indicated by (a) a stable mass detected by the EQCM and (b) by a measured FeCO₃ supersaturation value around 10 when the driving force for FeCO₃ precipitation diminishes. The acetic acid was injected as a buffered solution, to avoid a change of pH in the cell and to differentiate the effect of acetic acid from the effect of pH on FeCO₃ dissolution.

Table 1
Experimental conditions for FeCO₃ precipitation on polarized platinum coated quartz crystal at different pH values

Test solution	Deionized water + 0.1 wt.% NaCl
Test material	Platinum coated EQCM quartz crystal
Temperature	80°C
Total pressure of CO ₂	1 bar
Undissociated organic acid	None
Initial pH	6.6, 6.3, 6.0
Rotation velocity	Static conditions

Table 2
Experimental conditions for FeCO₃ dissolution on polarized (-700mV) platinum coated quartz crystal at different acetic acid concentrations

Test solution	Deionized water + 0.1 wt.% NaCl
Test material	Platinum coated EQCM quartz crystal
Temperature	80°C
Total pressure of CO ₂	1 bar
Undissociated (free) organic acid	1, 3 and 5 mM
Initial pH	6.0
Rotation velocity	Static conditions

RESULTS

I. FeCO₃ precipitation ³

The first set of experiments sought to determine what influence did the bulk pH have on FeCO₃ precipitation onto a platinum substrate. It is well known that higher values of bulk pH lead to higher FeCO₃ supersaturation, what favors the formation of FeCO₃ on steel. Temperature speeds up the kinetics, leading to a more dense and protective FeCO₃ layer. However, since it was here decided to use a platinum substrate, instead of iron, it was important to evaluate the factors that could affect the FeCO₃ precipitation.

Figure 2 shows the mass gain during FeCO_3 precipitation that occurred on a polarized platinum coated crystal for the three different values of pH. The kinetics and the gain in mass measured by the quartz crystal microbalance for pH 6.6, 6.3 and 6.0 was similar: 1.6, 1.5 and 1.7 $\text{mg}\cdot\text{cm}^{-2}$, respectively. The associated drop in bulk pH and FeCO_3 supersaturation (SS) during the experiments (shown in Table 3) is to be expected, due to the formation of the FeCO_3 layer.

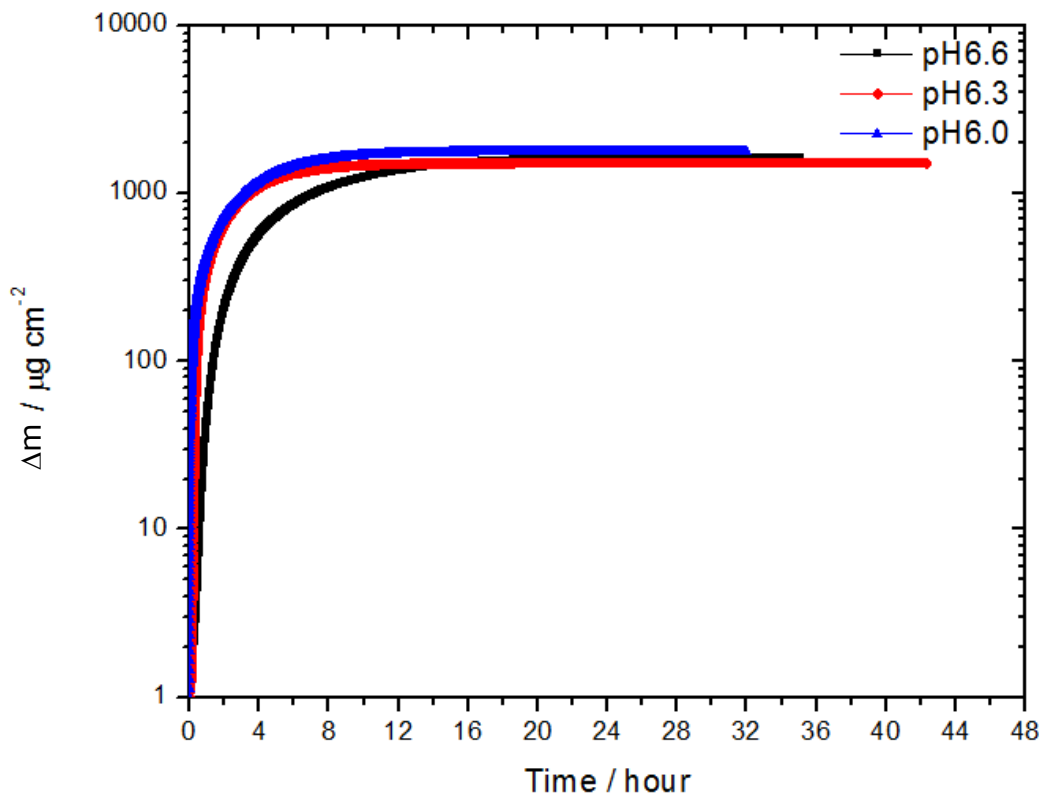


Figure 2: Mass gain during FeCO_3 precipitation on a polarized platinum coated quartz crystal at different bulk pH values (80°C , 0.1 wt.% NaCl and $\text{pCO}_2=0.53$ bar).

Table 3
Summary of experimental results for the FeCO_3 precipitation on a polarized (-700mV) platinum coated quartz crystal at different bulk pH values (80°C , 0.1 wt.% NaCl and $\text{pCO}_2=0.53$ bar), corresponding to Figure 2

pH		Fe^{2+} /ppm		SS(FeCO_3)		$\Delta m / \mu\text{g cm}^{-2}$	
Initial	Final	Initial	Final	Initial	Final	Initial	Final
6.6	6.6	32	1.5	300	12.8	0	1620
6.3	6.0	126	9	300	5.1	0	1523
6.0	5.4	547	506	300	16	0	1757

The SEM images (Figure 3) show either “plate” or “prism” shaped crystals of FeCO_3 depending on solution pH. The surface from the test at pH 6.6 shows well packed prisms, while the one at pH 6.3 shows a combination of prisms and plates. However, at pH 6.0 only plates were observed. Figure 4 shows the EDS analysis of the layer formed on the platinum crystal. The analysis shows the peaks of Fe, O, and C, consistent with the formation of FeCO_3 . XRD confirmed the previous finding that FeCO_3 was the sole “corrosion” product in these experiments.^{1,3}

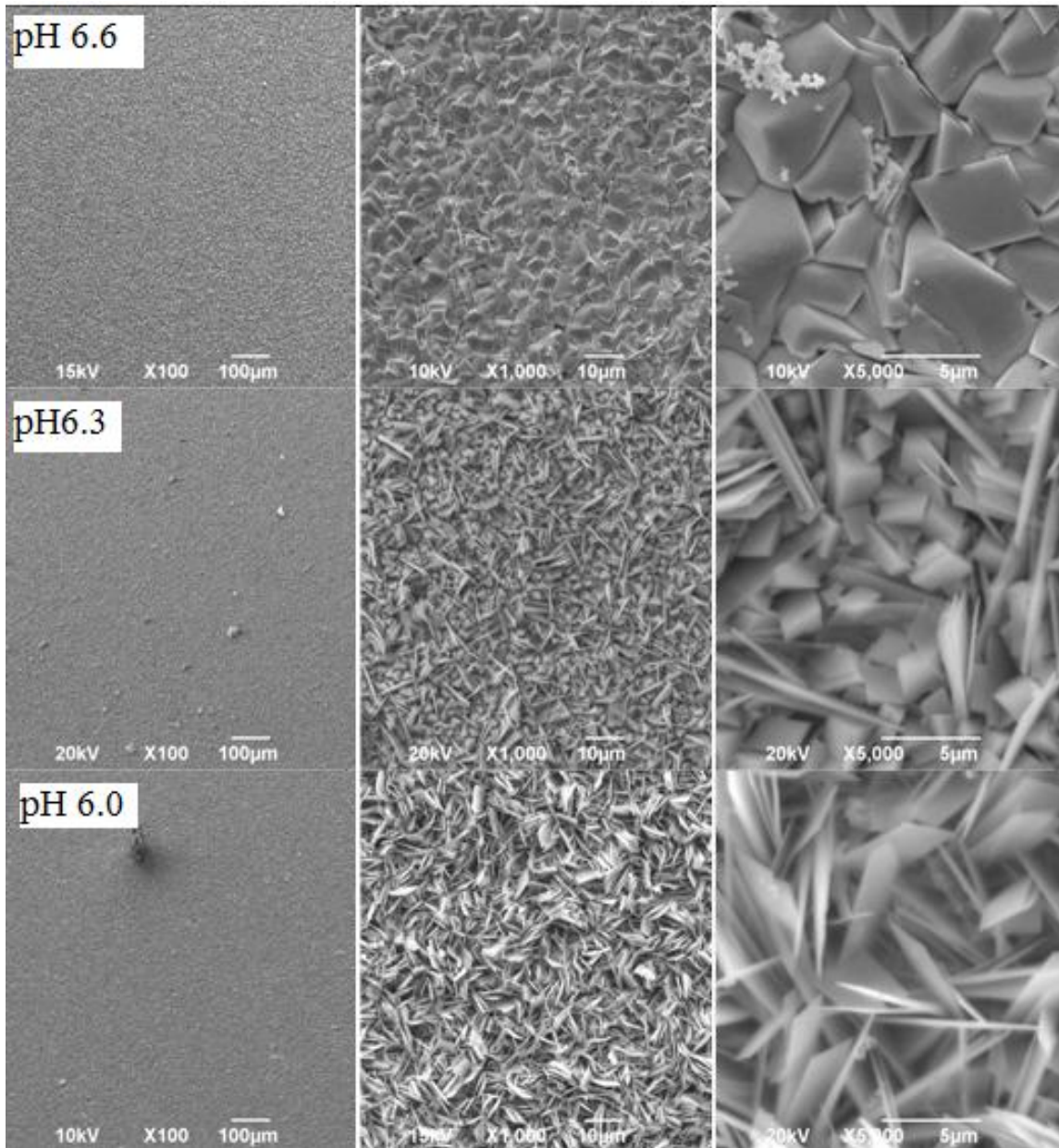


Figure 3: SEM images of FeCO_3 layers formed on polarized platinum coated quartz crystals at different pH values (80°C , 0.1 wt.% NaCl, $p\text{CO}_2=0.53$ bar).

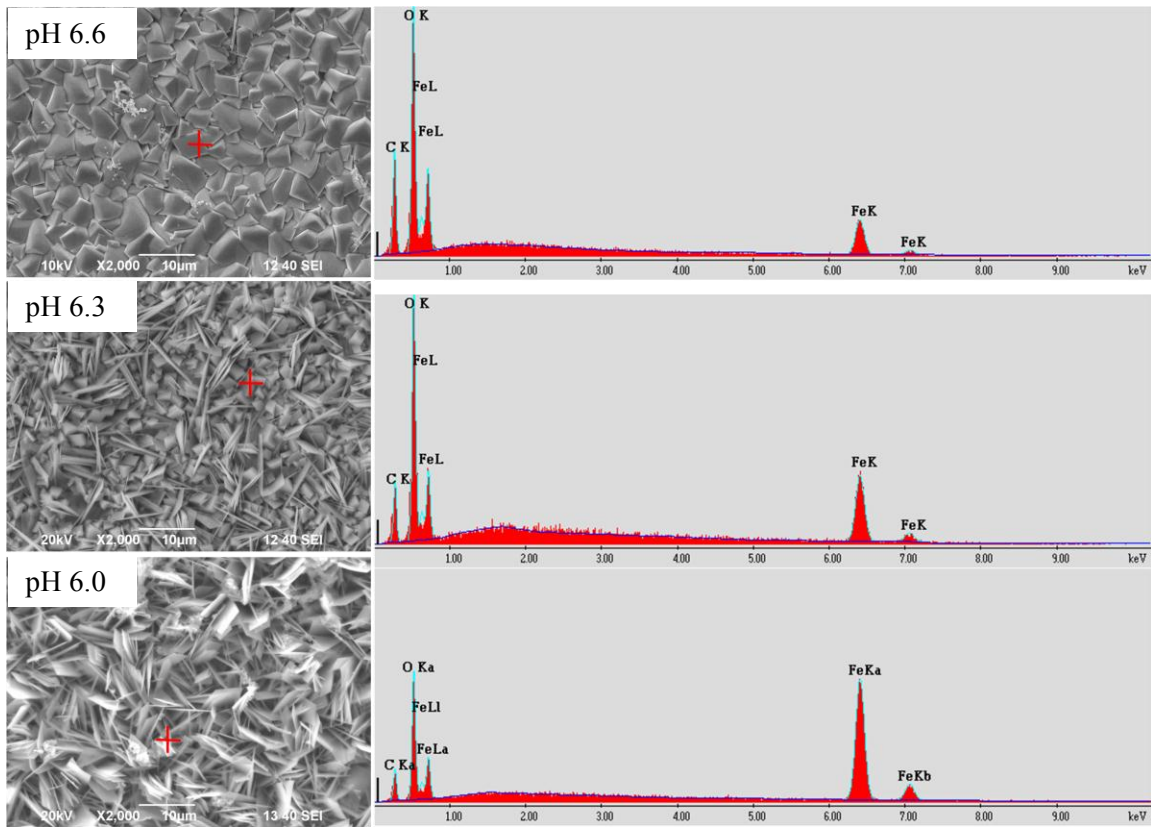


Figure 4: EDS analysis of FeCO_3 layers formed on polarized platinum coated quartz crystals at different pH values (80°C , 0.1 wt.% NaCl, $p\text{CO}_2=0.53$ bar).

These results match perfectly with the Raman spectroscopy and XPS analysis. Figure 5 and Figure 6 show the optical image and the Raman spectra for the FeCO_3 layers formed on platinum coated EQCM crystals at the three different pH values. A specific spot was selected for the optical image in the experimental data: prisms for pH 6.6 and 6.3 and plates for pH 6.0. The Raman spectra for those spots show two main vibrational modes at 292 and 1087 wavenumbers, which match the existing data in the literature for FeCO_3 (siderite).

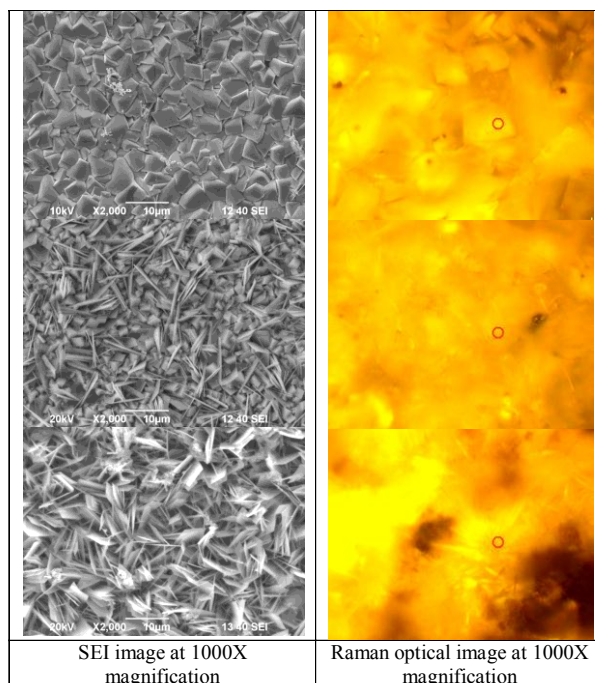


Figure 5: Raman optical image analysis of the FeCO₃ layers formed on polarized platinum coated quartz crystals at pH 6.6, pH 6.3, and pH6.0, arranged from top to bottom, respectively (80°C, 0.1 wt.% NaCl, and pCO₂=0.53 bar).

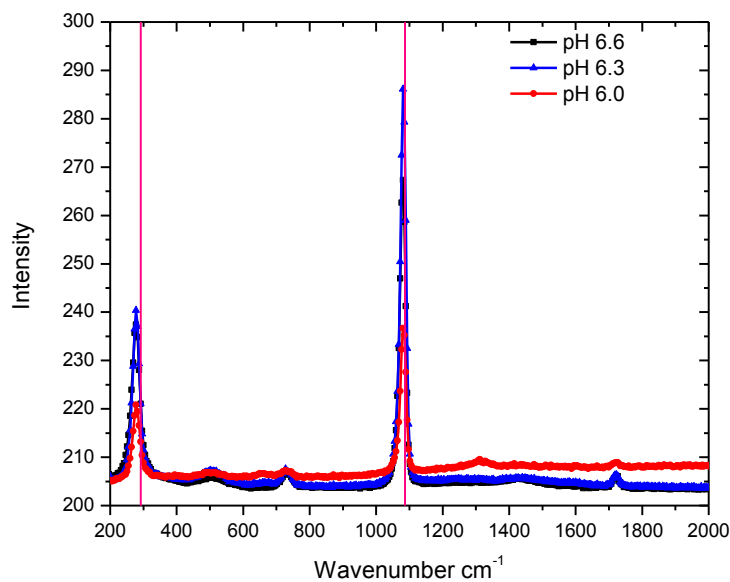


Figure 6: Raman spectra of the FeCO₃ layers formed on polarized platinum coated quartz crystals at different pH values (80°C, 0.1 wt.% NaCl, pCO₂=0.53 bar).

XPS corroborates the composition of an FeCO₃ layer on the platinum coated crystal (Figure 7). The experimental results were compared with the binding energies reported by J. K. Heuer in 1999⁴. Table 4 shows the comparison between the experimental results and the data reported in the literature by Heuer which verifies the composition of the FeCO₃ layer precipitated on the platinum coated crystal⁴. This leads to the first conclusion: that while the morphology of the crystals appeared to be different at the three different pH values, the composition of the layer precipitated on the platinum coated crystal is the same - FeCO₃ (siderite).

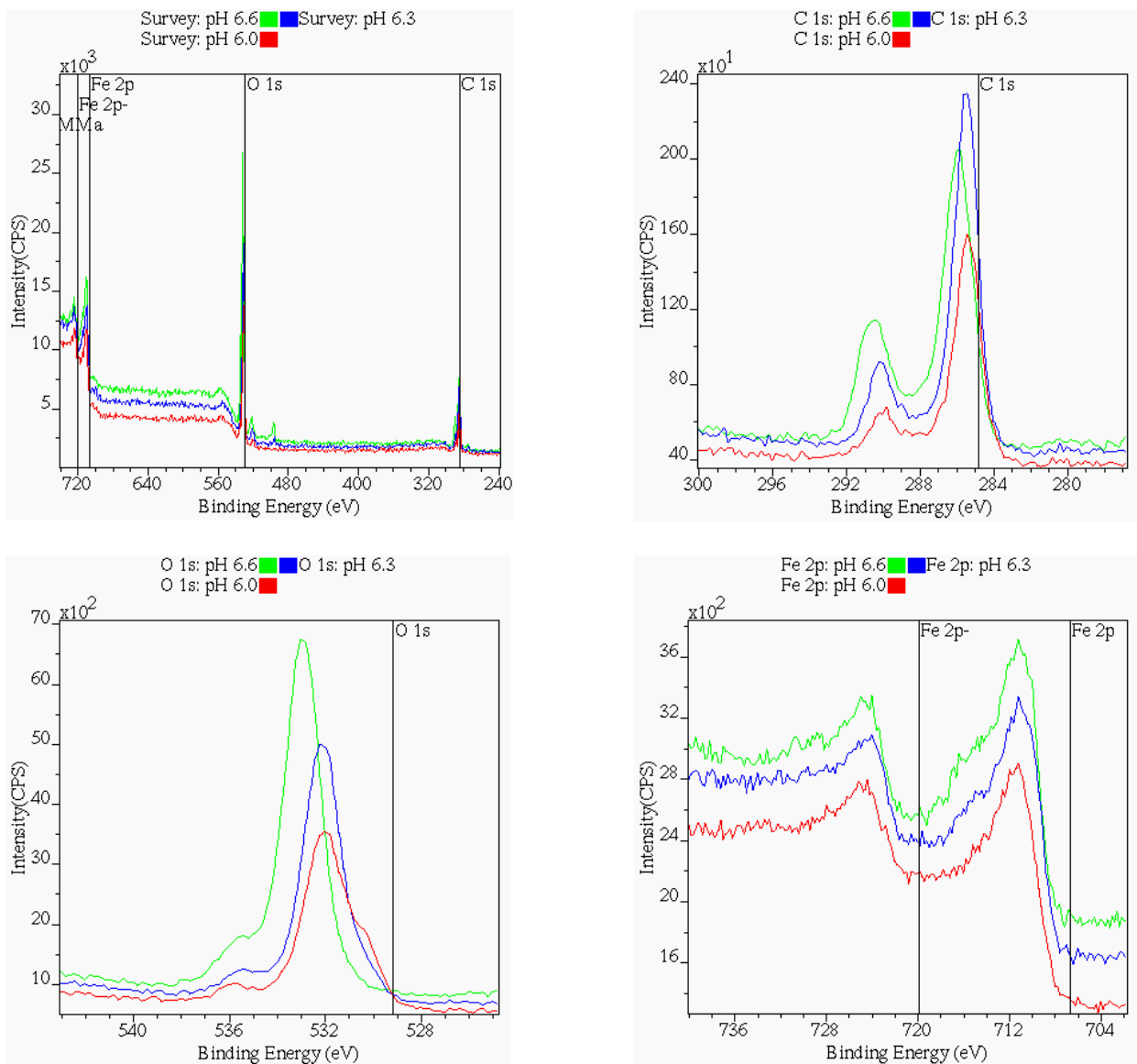


Figure 7: XPS scans of FeCO₃ layers formed on polarized platinum coated quartz crystals at different pH values (80°C, 0.1 wt.% NaCl, and pCO₂=0.53 bar)

**Table 4
Binding energies for FeCO₃⁴**

	Theoretical data				
	C 1s	O 1s	Fe 2p _{3,2}	Fe 2p _{1/2}	
	289.4	531.9	710.2	723.7	
	Experimental data				
	C 1s	O 1s	Fe 2p _{3,2}	Fe 2p _{1/2}	
	pH 6.6	285.8	532.9	711.6	724.8
	pH 6.3	285.7	532.0	710.9	724.5
pH 6.0	284.8	532.0	711.4	724.8	

Since this research sought primarily to investigate the solubility of FeCO_3 in the presence of acetic acid, it was necessary to narrow down the experimental conditions for FeCO_3 precipitation. Whereas previously the test matrix allowed for three different pH during FeCO_3 formation (see Table 1), similar results were obtained and therefore the initial pH 6.0 was used in all further experiments (see Table 5). The initial plan was to add acetic acid as a buffered solution in order to avoid the simultaneous change in pH. The buffer solution is more effective when the pH to pKa ratio is close to 1⁵. However, it is also practical to use a pH range of approximately ± 1 with respect to the pKa. Since the dissociation constant of acetic acid at 80°C is 4.86, it is better to work at an initial pH of 6.0 since this pH will decrease to around 5.4, in the range where the buffer solution is most effective. A large number of experiments were performed in order to evaluate the reproducibility of the FeCO_3 precipitation at pH 6.0, 80°C and 0.1 wt.% NaCl.

Table 5
Experimental conditions – FeCO_3 precipitation at pH 6.0

Test solution	Deionized water + 0.1 wt.% NaCl
Test material	Platinum coated EQCM quartz crystal
Temperature	80°C
Total pressure of CO_2	1 bar
Undissociated (free) organic acid	None
Initial pH	6.0
Rotation velocity	Static conditions

For the purpose of this study, three repeats of the same experiment were selected and labeled R1, R2 and R3. Figure 8 shows that the gain in mass for R1, R2 and R3 are very close to each other, approximately $1.5 \text{ mg}\cdot\text{cm}^{-2}$. The pH dropped to around 5.4 in all the experiments as a result of the FeCO_3 precipitation. Consequently, the saturation value (SS) of FeCO_3 also decreased. The SEM images for R1, R2 and R3 show mostly plates with a few prisms on the top of the plates (Figure 9). EDS analyses of the layer formed on the polarized platinum coated crystal confirms the presence of C, Fe and O constituent elements for FeCO_3 as shown in Figure 10. XPS analyses corroborated this observation. Therefore, these experiments prove that is possible to successfully reproduce the FeCO_3 precipitation on polarized platinum coated crystal, at the given set of conditions.

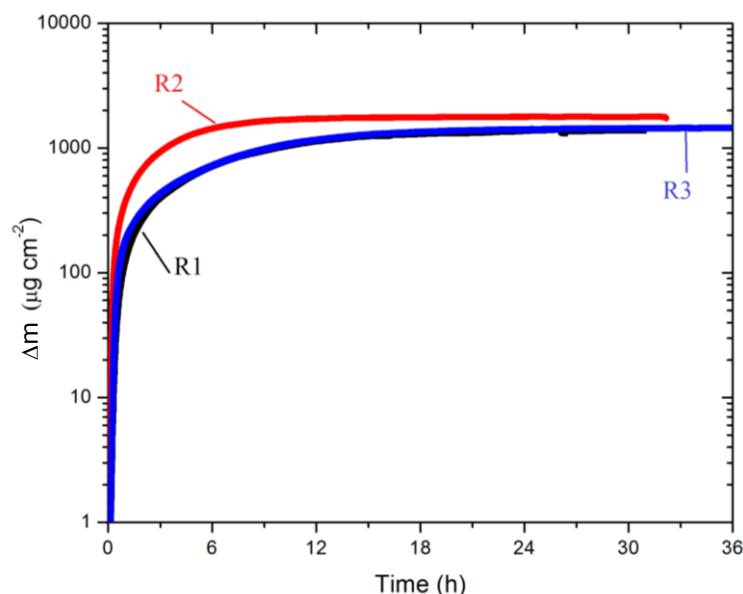


Figure 8: R1, R2 and R3 represent the reproducibility of the mass gain for FeCO_3 precipitation tests on polarized platinum coated quartz crystals at pH 6.0, 80°C, 0.1 wt.% NaCl, and $p\text{CO}_2=0.53$ bar.

©2013 by NACE International.

Requests for permission to publish this manuscript in any form, in part or in whole, must be in writing to NACE International, Publications Division, 1440 South Creek Drive, Houston, Texas 77084.

The material presented and the views expressed in this paper are solely those of the author(s) and are not necessarily endorsed by the Association.

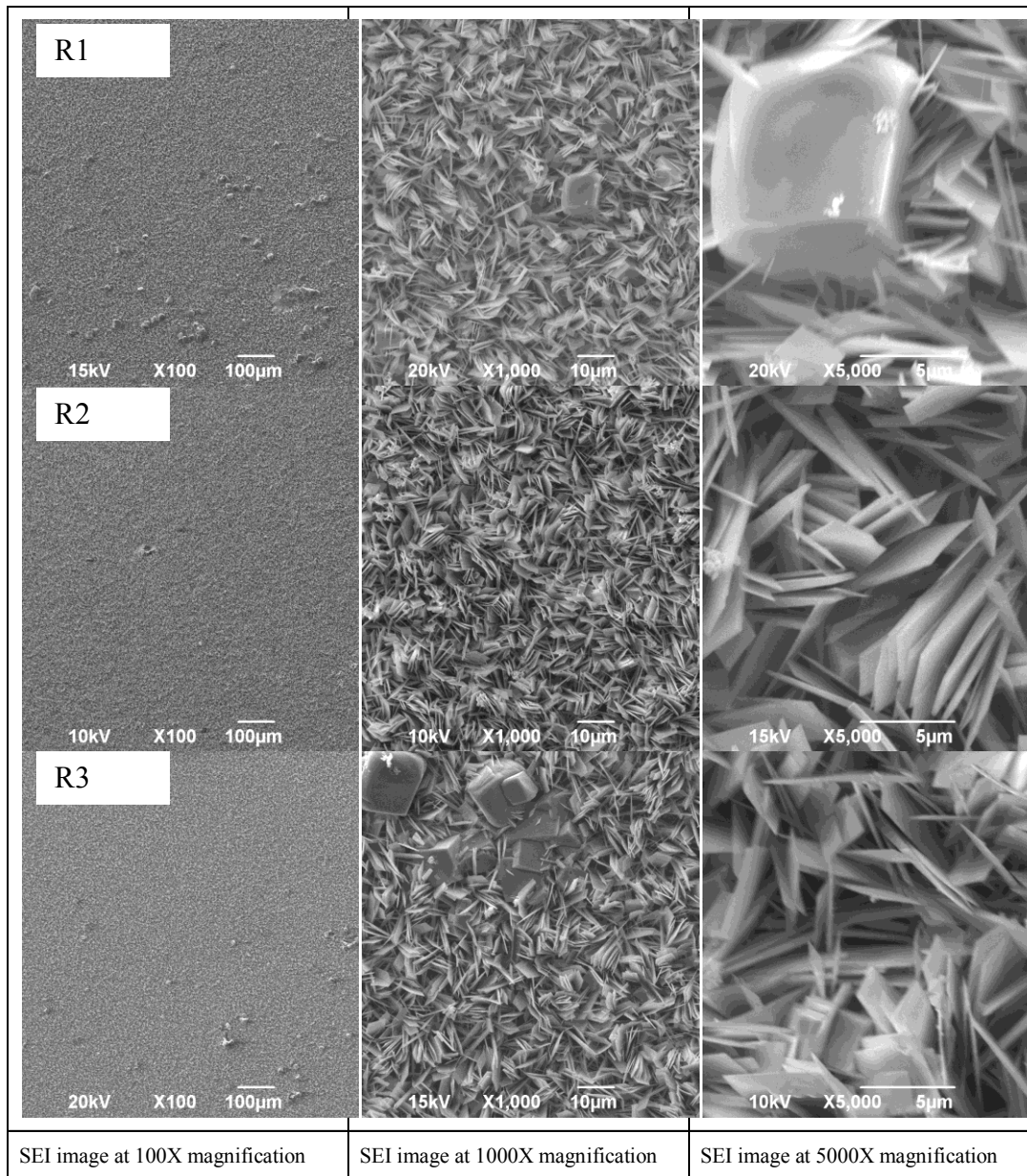


Figure 9: SEM images of FeCO_3 layers formed on polarized platinum coated EQCM quartz crystals at pH 6.0, 80°C, 0.1 wt.% NaCl, and $p\text{CO}_2=0.53$ bar.

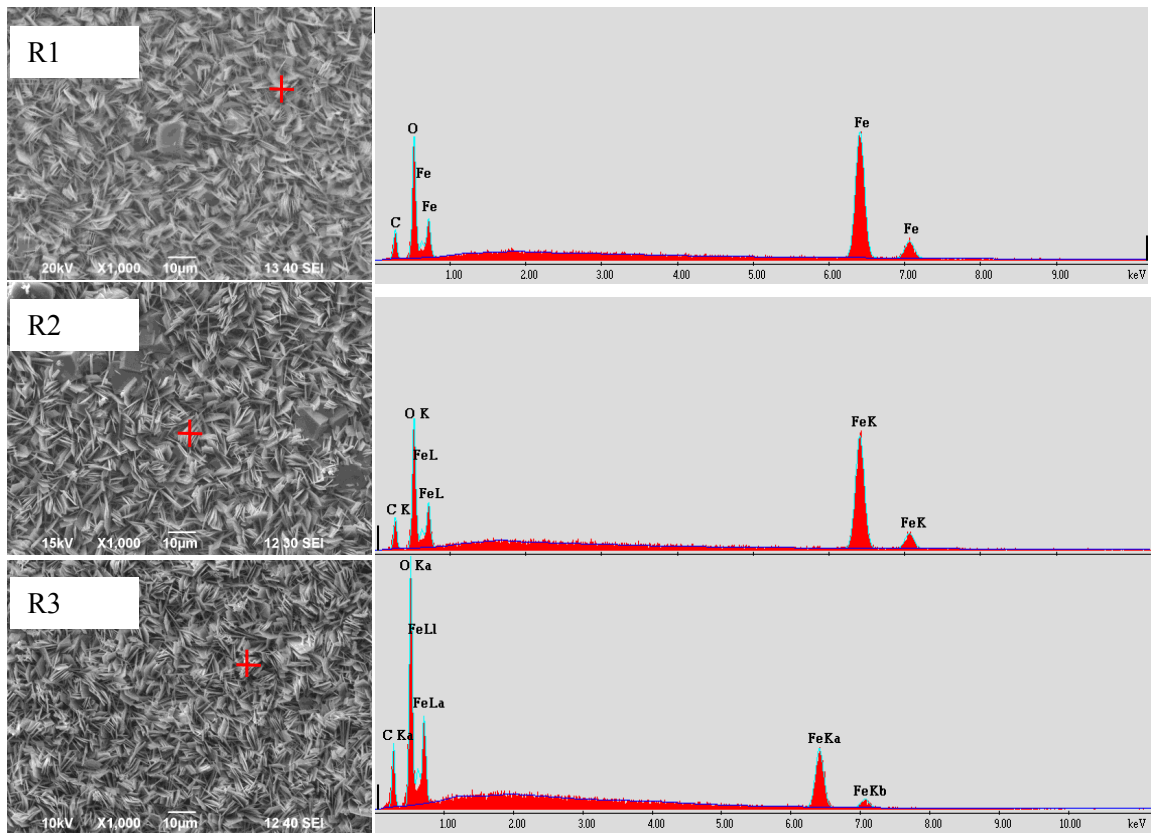


Figure 10: EDS analysis of FeCO_3 layers formed on polarized (-700mV) platinum coated EQCM quartz crystals at pH 6.0, 80°C, 0.1 wt.% NaCl, and $\text{pCO}_2=0.53$ bar.

II. FeCO_3 dissolution by acetic acid³

The EQCM was used to evaluate the dissolution kinetics of FeCO_3 due to the presence of different amounts of undissociated buffered acetic acid solution at 80°C, an initial pH 6.0, 0.1 wt.% NaCl, initial $\text{SS}(\text{FeCO}_3)$ of 200 and $\text{pCO}_2=0.53$ bar. The results in Figure 11 show that the presence of acetic acid at a constant pH led to a partial dissolution of the FeCO_3 , as indicated by a decrease in the measured mass of the FeCO_3 . The span between the vertical lines represents the period of time during which the designated amount of acid was added into the solution.

Table 6 shows the change in mass per unit area (Δm), pH, iron concentration (Fe^{2+}), and supersaturation value of FeCO_3 , $\text{SS}(\text{FeCO}_3)$, at points I, II, III, and IV for each graph in Figure 11 a, b, and c.

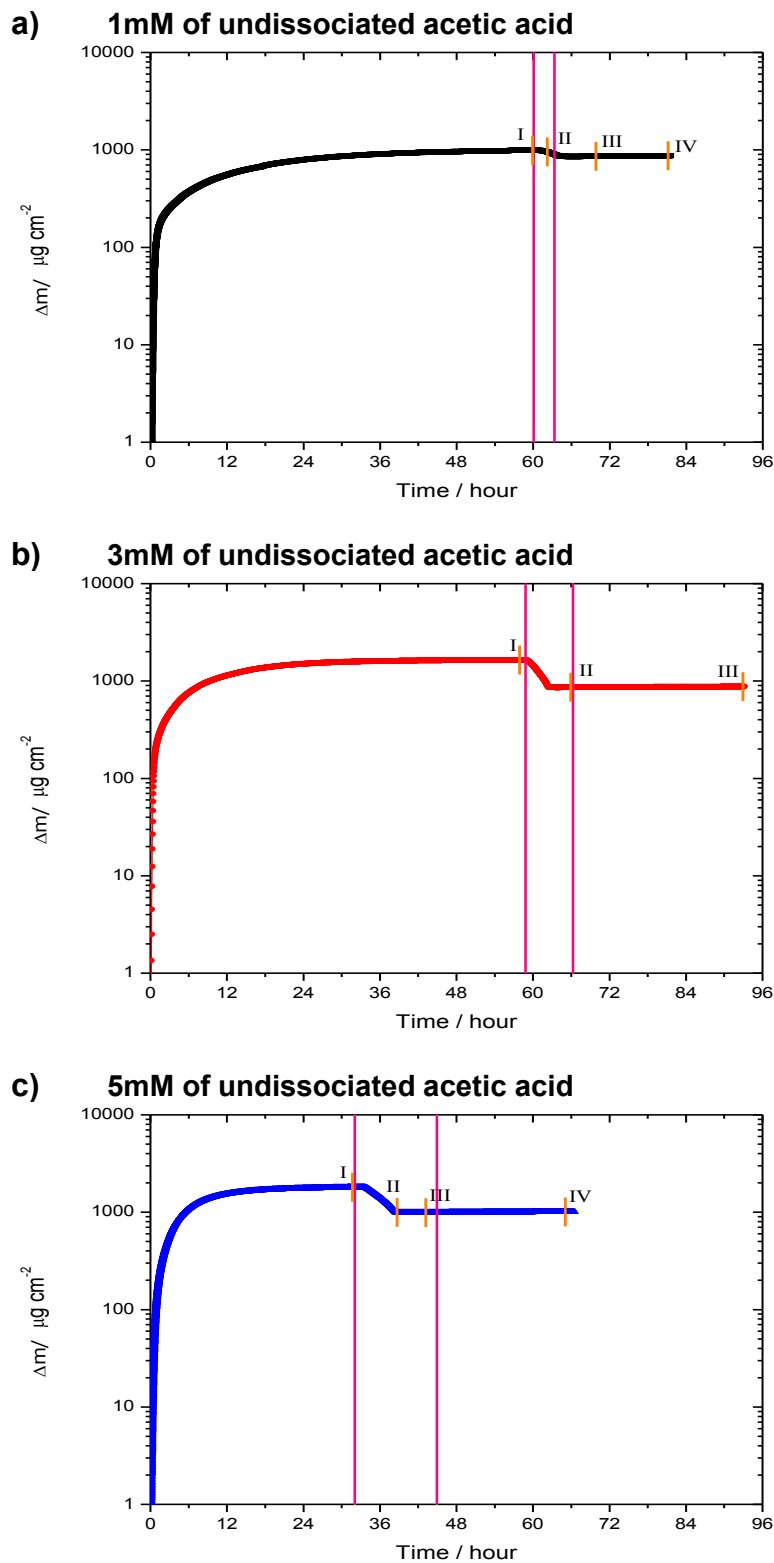


Figure 11: FeCO_3 precipitation-dissolution studies on polarized (-700mV) platinum coated EQCM quartz crystals at different undissociated acetic acid concentrations (80°C, 0.1 wt.% NaCl, $p\text{CO}_2=0.53$ bar).

Table 6
Experimental results of the FeCO₃ dissolution in the presence of different concentrations of acetic acid.

1mM of undissociated acetic acid				
Period of time	Δm ($\mu\text{g cm}^{-2}$)	pH	Fe ²⁺ (ppm)	SS(FeCO ₃)
I	989	5.4	343	13
II	955	5.3	355	9.16
III	859	5.3	294	6.32
IV	873	5.2	392	7
3mM of undissociated acetic acid				
Period of time	Δm ($\mu\text{g cm}^{-2}$)	pH	Fe ²⁺ (ppm)	SS(FeCO ₃)
I	1639	5.4	347	11.1
II	866	5.2	291	4.6
III	875	5.2	270	3.9
5mM of undissociated acetic acid				
Period of time	Δm ($\mu\text{g cm}^{-2}$)	pH	Fe ²⁺ (ppm)	SS(FeCO ₃)
I	1797	5.4	284	10.5
II	994	5.1	308	3.6
III	991	5.1	341	4.2
IV	1006	5.1	290	2.9

The loss of FeCO₃ at 1, 3 and 5mM was 11%, 46% and 44%, respectively, for the entire surface (Figure 12). The SEM shows that the FeCO₃ plates which initially formed on the platinum quartz crystal dissolved and only prisms remained (Figure 13). These prisms were not clearly visible in the SEM image following the FeCO₃ precipitation at pH 6.0 (Figure 13). Two possible things may have occurred: 1) dissolution of the plate shaped FeCO₃ crystals leaving the prism shaped crystals behind or 2) Ostwald ripening occurred. If the first mechanism is correct, it may follow that the plates (which are smaller/younger crystals) are less stable and, therefore, more easily dissolved by the addition of the acetic acid, so that the prisms were all that remained. The second mechanism, Ostwald ripening, refers to a spontaneous process of crystal enlargement which occurs because smaller crystals are kinetically favored (nucleate more easily and are energetically less stable), while large crystals are thermodynamically favored (represent a lower energy state). Small crystals will attain a lower energy state if transformed into larger crystals⁶. Either mechanism could explain the presence of the prisms remaining on the platinum coated crystal.

Although these two possible mechanisms can be used to explain why there was a point at which the dissolution process stopped even though the acid was still being added, it is more likely that the acetic acid has a "preference" for certain crystal morphologies which it can more easily dissolve, as was reported for the case of calcite-type calcium carbonate (CaCO₃). The mechanism of Ostwald ripening would be expected to develop larger crystals, and this is not supported by comparison of the SEM images in Figure 13. Since both CaCO₃ (as calcite) and FeCO₃ (as siderite) belong to the same crystal structure family of carbonates, the different rate of dissolution observed for varying CaCO₃ morphologies can be generalized and extended for FeCO₃. For example, plate-like CaCO₃ will easily dissolve in HCl as compared to more oblong prismatic crystals of CaCO₃. This may explain why the measured mass loss (dissolution of FeCO₃) stopped in spite of the continued addition of buffered acetic acid as shown in Figure 11.

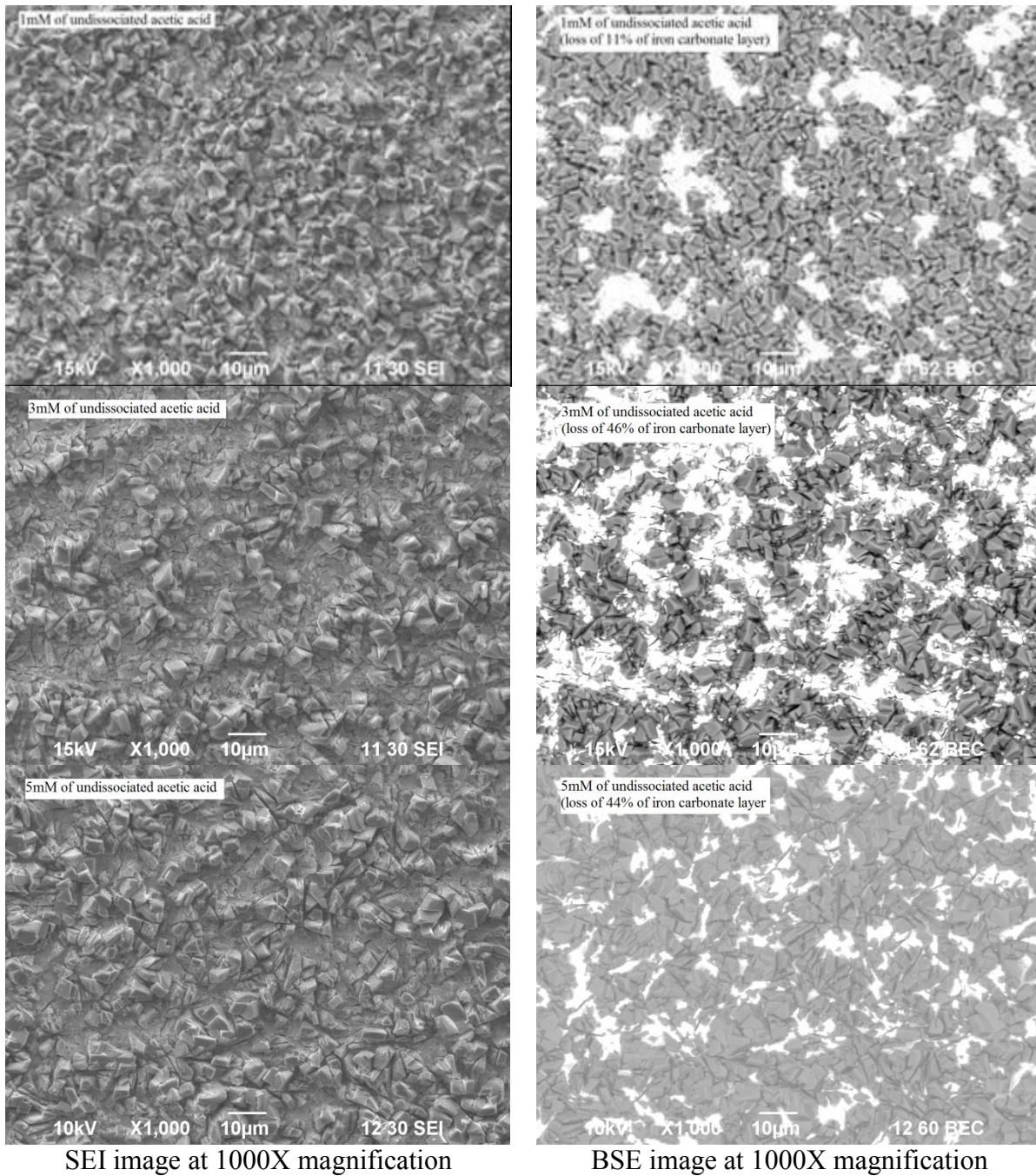


Figure 12: SEM and associated backscatter images of FeCO_3 layers after dissolution due to the presence of free acetic acid at 1mM, 3mM, and 5mM concentrations (pH 6.0, 80°C, 0.1 wt.% NaCl, and $\text{pCO}_2=0.53$ bar).

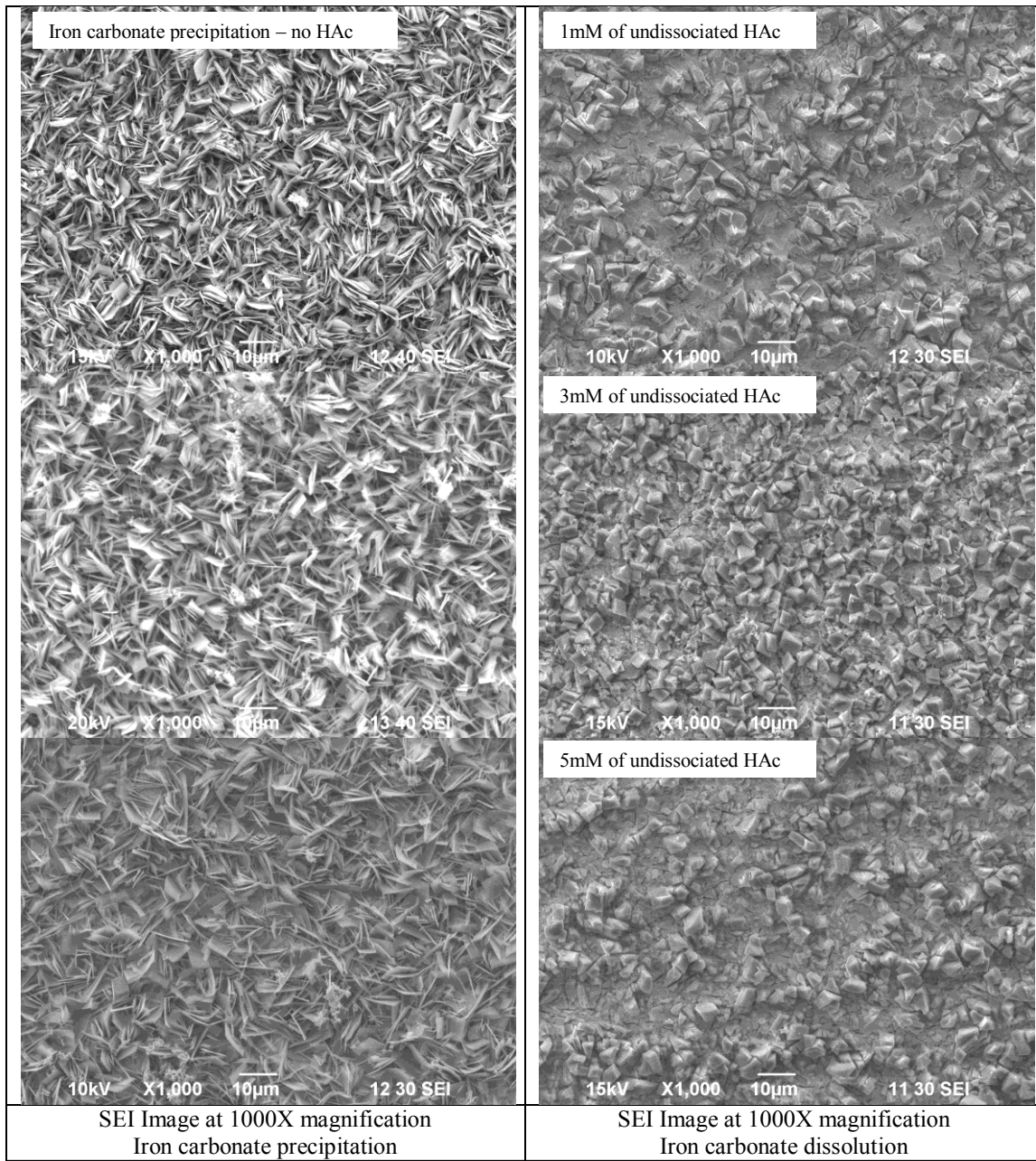


Figure 13: SEM images of FeCO_3 precipitation layer before and after dissolution by addition of acetic acid at 1mM, 3mM, and 5mM concentrations (pH 6.0, 80°C, 0.1 wt.% NaCl, and $\text{pCO}_2=0.53$ bar).

As the addition of different amounts of acetic acid yielded similar results, the following discussion will use the 3mM addition as being representative of the three experiments. In Figure 14 it can be observed that the buffered acetic acid solution dissolves the FeCO_3 layer in the first few hours, even while the acid is still being injected.

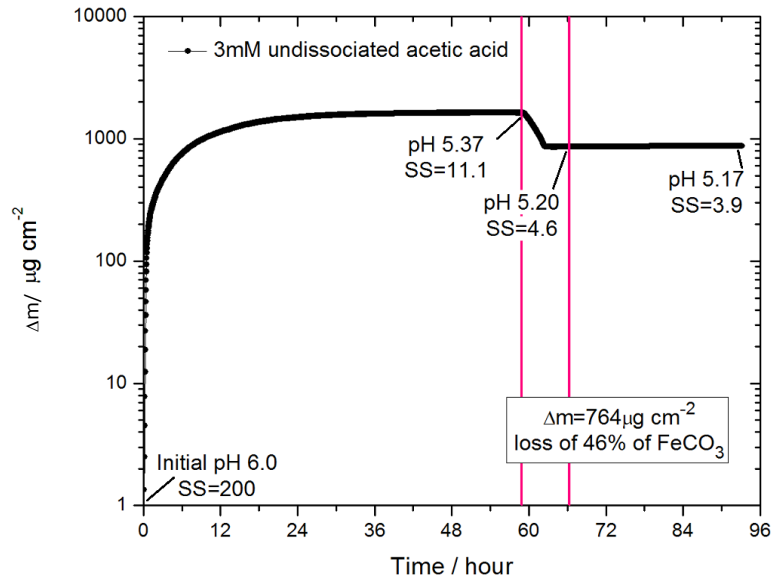


Figure 14: Measured FeCO_3 precipitation and dissolution on polarized (-700mV) platinum coated EQCM quartz crystal (3mM of undissociated acetic acid at 80°C , 0.1 wt.% NaCl, and $\text{pCO}_2=0.52$ bar).

EDS analysis of the prisms shows the presence of Fe, C, and O, the constituent elements for FeCO_3 . Further analysis of the exposed area revealed the presence of platinum in addition to Fe, C, and O (Figure 15). This means there is a thin layer formed on the exposed substrate, otherwise it would not be possible to see these peaks, even though the intensity is low. The EDS reveals the presence of the platinum because the electron beam can easily penetrate the layer formed on the platinum coated crystal.

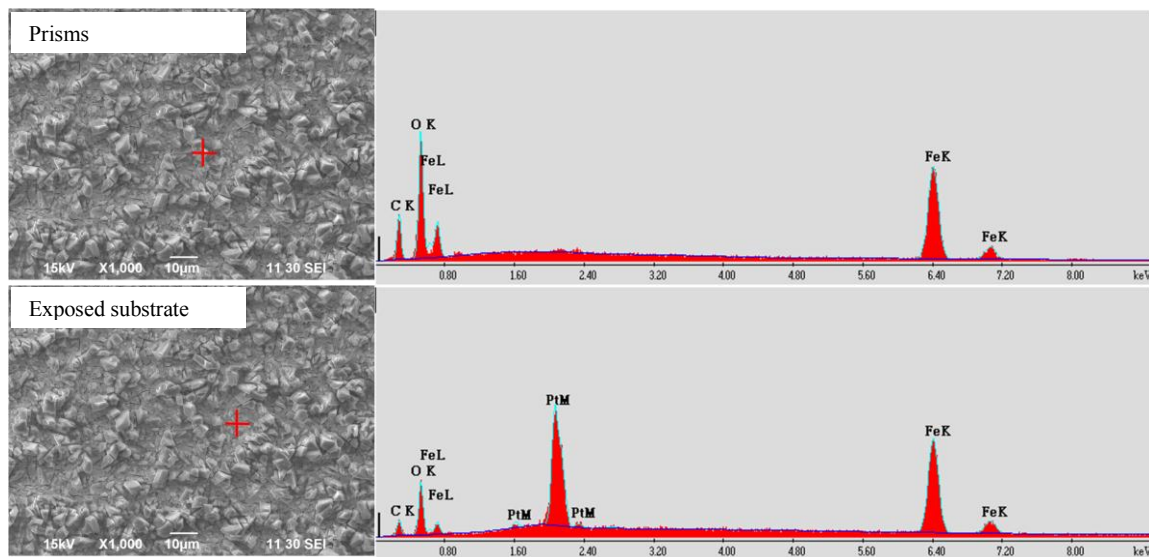


Figure 15: EDS analysis of FeCO_3 layers formed on polarized platinum coated quartz crystals at pH 6.0, 80°C , 0.1 wt.% NaCl, $\text{pCO}_2=0.53$ bar and 3mM of undissociated acetic acid.

The Raman spectra and associated optical image for the sample exposed to 3mM of undissociated acetic acid is shown in Figure 16. Two areas were analyzed: the prisms and the exposed area. Both areas show the main peaks of FeCO_3 . The surface analysis performed by Raman spectroscopy requires the presence of a dense corrosion product layer. As the vibrational spectrum of the substrate is dominant, Raman spectroscopy is an inappropriate method for analysis of the thin layer that remains after the addition of the buffered acetic acid solution.

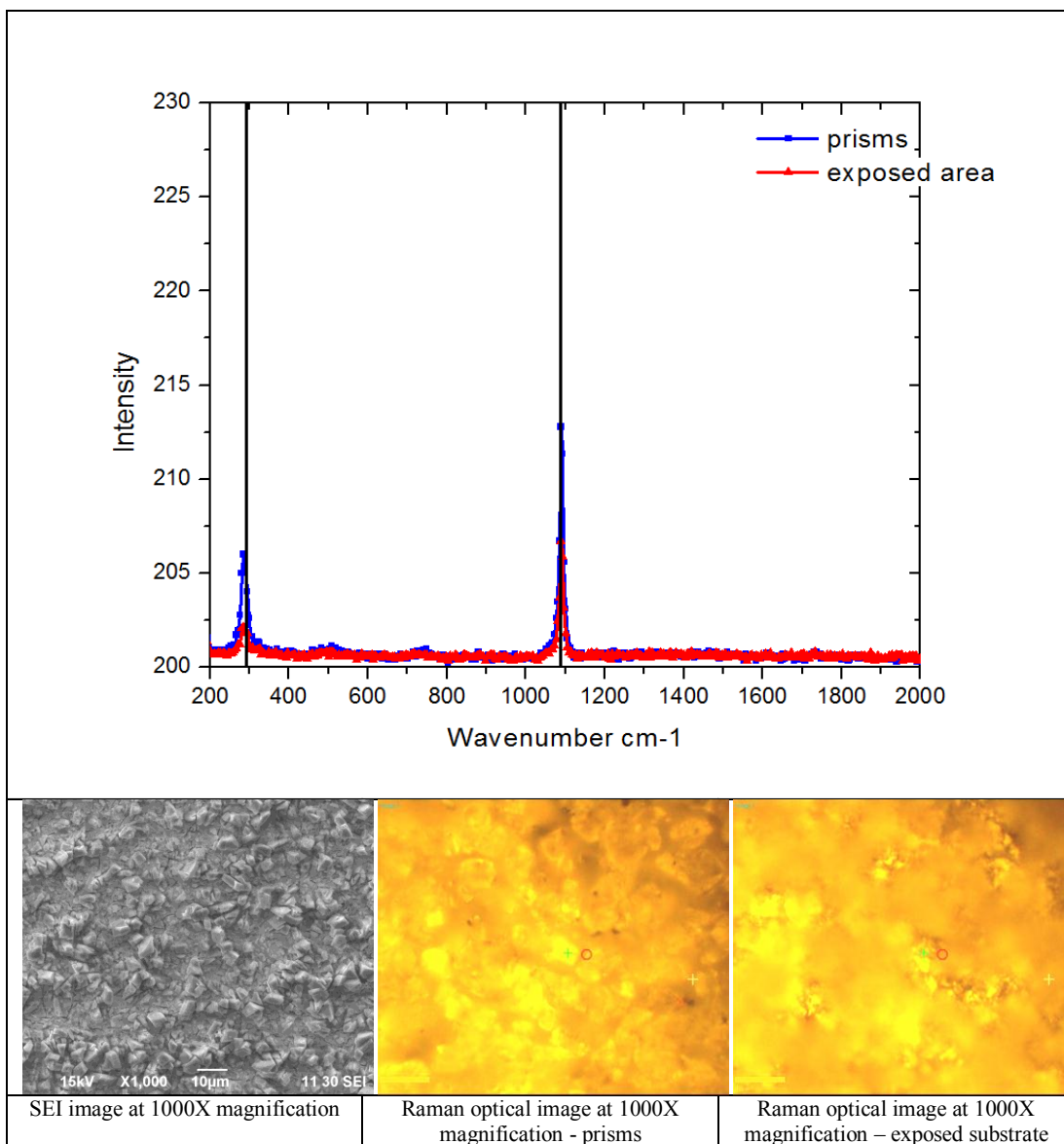


Figure 16: Raman spectra and optical image of the FeCO_3 layer formed on polarized platinum coated quartz crystal at 80°C , 0.1 wt.% NaCl, $p\text{CO}_2=0.53$ bar and 3mM of undissociated acetic acid.

X-ray photoelectron spectroscopy (XPS) scans of the FeCO_3 layer formed on polarized (-700mV) platinum coated quartz crystals (80°C , 0.1wt.% NaCl, $p\text{CO}_2=0.53$ bar) were performed before and after the addition of 3mM of undissociated acetic acid, as shown in Figure 17. The results match the binding energies of FeCO_3 at 298.8 for C 1s, 532 for O 1s, 711 for Fe $2p_{3,2}$ and 724.8 for Fe $2p_{1/2}$. It was important to analyze the remaining prismatic crystals by a different analytical technique to prove that FeCO_3 was the deposit (layer) formed on the platinum substrate. TEM/EDS and electron diffraction patterns confirmed this conclusion, as shown in Figure 18 and Figure 19.

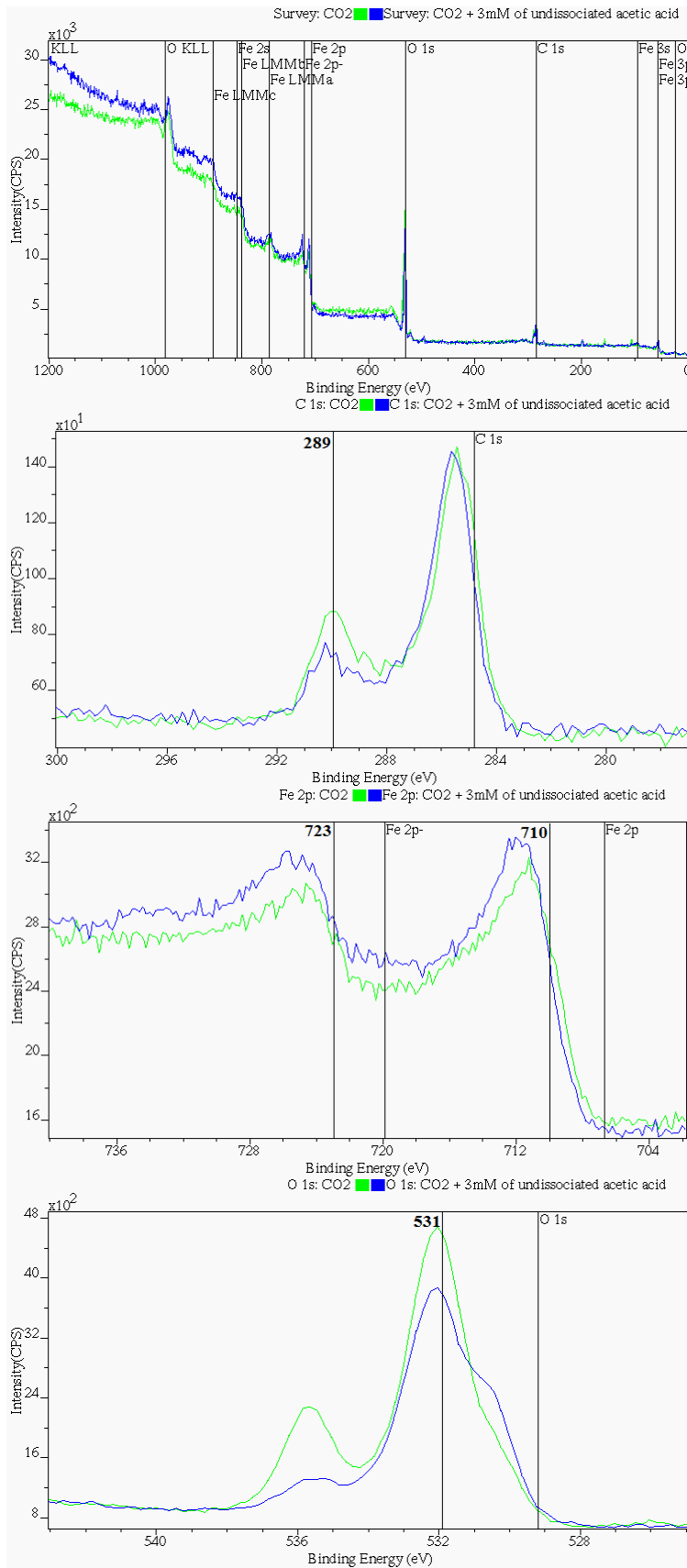


Figure 17: XPS scans of FeCO₃ dissolution on polarized platinum coated quartz crystal in the presence of acetic acid (80°C, 0.1 wt.% NaCl, and pCO₂=0.53 bar)

©2013 by NACE International.

Requests for permission to publish this manuscript in any form, in part or in whole, must be in writing to NACE International, Publications Division, 1440 South Creek Drive, Houston, Texas 77084.

The material presented and the views expressed in this paper are solely those of the author(s) and are not necessarily endorsed by the Association.

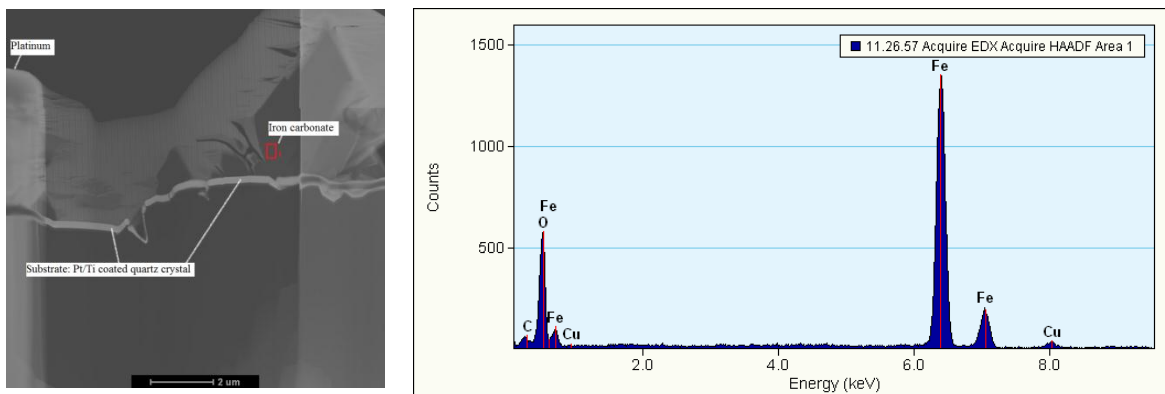


Figure 18: TEM image and EDS analysis of FeCO₃ plates formed on polarized platinum coated quartz crystal in the presence of 3mM of undissociated acetic acid (80°C, 0.1 wt.% NaCl, and pCO₂=0.53 bar).

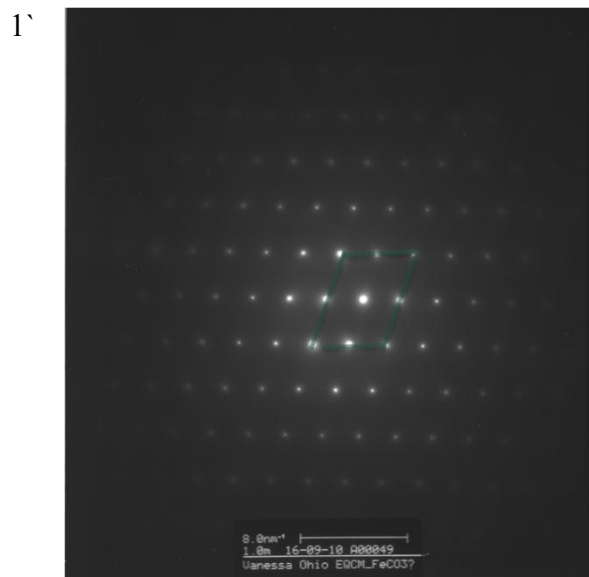


Figure 19: TEM image and ED data of the prisms found on polarized platinum coated quartz crystal in the presence of 3mM of undissociated acetic acid (80°C, 0.1 wt.% NaCl, and pCO₂=0.53 bar).

CONCLUSIONS

It was found that:

- A polarized platinum substrate can be used to develop a repeatable FeCO₃ precipitation layer for analysis and further testing.
- The morphology of an FeCO₃ precipitation layer on a platinum substrate varied over the pH range tested (pH 6.0 – pH 6.6), but the composition of the precipitated layer was determined to be the same for each case.
- The presence of acetic acid partially removed a protective FeCO₃ layer by selective dissolution influenced by crystal morphology.

ACKNOWLEDGEMENTS

The different surface analysis techniques were done in the Department of Physics and Astronomy at Ohio University under the supervision and guidance of Dr. Ingram, Dr. Martin Kordesch and Dr. Aurangzeb Khan. The Department of Materials Science and Engineering in CASE Western Reserve University, under Dr. Amir Avishai's supervision, was also instrumental in allowing me to complete this project. In particular, Dr. Kordesch provided valuable feedback on the electron diffraction data analysis.

©2013 by NACE International.

Requests for permission to publish this manuscript in any form, in part or in whole, must be in writing to NACE International, Publications Division, 1440 South Creek Drive, Houston, Texas 77084.

The material presented and the views expressed in this paper are solely those of the author(s) and are not necessarily endorsed by the Association.

REFERENCES

1. Fajardo, V., Canto, C., Brown, B., and Nestic, S., "The Effect of Acetic Acid on the Integrity of Protective Iron Carbonate Layers in CO₂ Corrosion of Mild Steel."CORROSION/08, paper no.08333. Houston, TX:NACE, 2008.
2. Yang, Y., Brown, B., and Srdjan, N., "Application of EQCM to the Study of CO₂ Corrosion."October 6-10, paper no.Paper #4071,. Las Vegas, NV,:17th International Corrosion Congress, 2008.
3. Fajardo, V. "Localized CO₂ Corrosion in the Presence of Organic Acids."Master of Science, Ohio University,2011.
4. Heuer, J. K., and Stubbins, J. F., "An XPS Characterization of FeCO₃ Films from CO₂ Corrosion." Corrosion Science 41, 7(1999): p. 1231-1243.
5. Silberberg, M.S. *Chemistry the Molecular Nature of Matter and Change*. 4th edition. Ohio, USA: McGraw Hill, 2006, pp. 1088.
6. West, A.R. *Solid State Chemistry and its Applications*. 10th edition. Great Britain: John Wiley & Sons, 1998, pp. 734.